JOURNAL OF MATERIALS SCIENCE: MATERIALS IN MEDICINE 9 (1998) 797–802

Identification and mapping of the amorphous phase in plasma-sprayed hydroxyapatite coatings using scanning cathodoluminescence microscopy

K. A. GROSS*‡†, M. R. PHILLIPS*
* *Microstructural Analysis Unit, and also* † *Department of Chemistry, Materials and Forensic Sciences, University of Technology, Sydney, Box 123, Broadway, New South Wales 2007, Australia*
E-mail: karlis.gross@eng.monash.edu.au

The presence and distribution of the amorphous phase is a key factor in the performance and bone-bonding behavior of plasma-sprayed hydroxyapatite coatings. Microanalysis of coatings was conducted with microprobe Raman and scanning cathodoluminescence microscopy. It was confirmed that the darker regions in polished cross sections represent the amorphous phase. The more intense cathodoluminescence emission from the amorphous phase during electron-beam irradiation compared with the crystalline phase was used to detect the two structurally different areas within the sample. By selecting the peak of the emission at 450 nm it was possible to raster the surface with the electron beam and produce a map of the amorphous phase in polished sections, a fracture surface and an as-sprayed surface of the plasma-sprayed coating. Cathodoluminescence microscopy, based on the different light emission from the amorphous phase and hydroxyapatite, is a useful tool for identifying and mapping of the amorphous-phase constituent in plasma-sprayed coatings.

1. Introduction

The performance of plasma-sprayed calcium phosphate coatings is very dependent upon the coating microstructure. An important aspect in coating development for biomedical applications is to ascertain the influence of the microstructure on coating longevity, the effect on bone growth and the ability to bond to osseous tissue. The amorphous phase is very often found in plasma-sprayed hydroxyapatite coatings and despite its ability to stimulate bone growth [1, 2] may also assist coating degradation [3, 4]. The presence and location of the amorphous phase is thus an important microstructural entity to identify both at the production stage and coating assessment in histological sections from animal and clinical studies. Typical methods used to measure the quantity of this phase have been restricted mainly to X-ray diffraction [5–7] which becomes exceedingly difficult with high crystallinity coatings. Other characterization methods are required to identify the amorphous phase.

Microanalysis techniques are necessary to study the coating and the bone at the microstructural level. Techniques such as microspectroscopic Fourier transform–infrared spectroscopy [8], microbeam X-ray diffraction [9], Raman microprobe [10] and electron microscopy [11–13] have been used previously to investigate different aspects of the coating and bone. Of these techniques, Raman microprobe and electron microscopy are techniques with the highest spatial resolution and can be used to study chemical phases at the micron level. Transmission electron microscopy requires significant sample preparation usually restricting the size of the sample to be studied. Scanning electron microscopy can accommodate larger samples; however, quantitative chemical information using energy dispersive X-ray analysis can only be gained usually at concentrations greater than 1 wt %.

Cathodoluminescence has been used primarily by geologists to identify the rare-earth impurities (for example Ce^{3+}, Sm^{3+}, Dy^{3+}, Tb^{3+}, Eu^{3+}, Eu^{2+}, Sm^{2+}, Mn^{2+}, etc.) in apatites [14–17]. This technique, which measures the light emission from a material after exposure to high-energy electrons, is capable of measuring impurities as low as 0.01 mol % in apatites [18]. Cathodoluminescence (CL) microscopy analysis is able to provide high spatial (lateral and depth) resolution information on the concentration and distribution of the chemical state (oxidation state and co-ordination) of impurities and point defects in a material. Therefore, the different atomic arrangements in the amorphous calcium phosphate and hydroxyapatite renders it suitable for CL analysis of plasma-sprayed

‡ Author to whom all correspondence should be addressed.
Present address: Department of Materials Engineering, Monash University, Clayton, VIC 3168, Australia.

hydroxyapatite coatings. In this study microprobe Raman as well as cathodoluminescence microscopy and microanalysis will be used to identify and locate the amorphous-phase constituent in polished sections, fracture surfaces and the as-sprayed surface of coatings made by plasma spraying hydroxyapatite.

2. Materials and methods

Two reference materials mounted in epoxy resin were used as standards to determine the cathodoluminescence emission upon irradiation with an electron beam. The hydroxyapatite sample was produced by heating a pressed body to 1200°C in flowing air bubbled through water prior to entering the furnace. The amorphous phase was produced by injecting hydroxyapatite powder with a particle size range of 10–40 μm in a Sulzer Metco (Westbury, New York, USA) 3MB plasma torch operated using argon and nitrogen as plasma-spray gases. A spraying distance of 15 cm was employed to encourage dehydroxylation and a fast torch traverse speed to prevent heating of the coating.

A coating produced at The Thermal Spray Laboratory, State University of New York at Stony Brook, was used as the initial coating for analysis. A part of the coating was crushed and the amorphous content calculated using an internal standard described elsewhere [19]. A Siemens (Karslruhe, Germany) D-5000 diffractometer operated in a theta–theta arrangement, employing CuK_α radiation generated at 40 kV and 30 mA, was used to determine the average amorphous content by analyzing a crushed coating segment. The antiscatter and detector slits were 2.0 and 0.2 mm, respectively, and the diffracted signal collected over a two theta range of 20°–60° with a step size of 0.02° and an acquisition time of 3 s per step.

The location of the amorphous phase was identified using two methods prior to cathodoluminescence analysis. Optical microscopy was used to locate the raised crystalline plateaus created by the preferential removal of the amorphous phase during polishing. This was confirmed by Raman microprobe spectroscopy performed on the same polished coating. Laser-Raman microanalysis was conducted on a DILOR *X–Y* Modular Laser Raman Spectrometer (Lille, France). Microstructural features were identified on a light microscope with a 100 × microscope objective. Routine analyses were conducted using the argon green line at 514.5 nm, with a laser power of 20 mW, exciting wavelength 514.532 nm. This output is within the range of power levels which do not incur any notable specimen damage [10]. A spectral slit width of 3.12 cm^{-1} was selected. Spectra from an irradiated area, using a spot diameter of 1 μm^2, were recorded within the range of 800 and 1200 cm^{-1} where the most intense peaks for hydroxyapatite and the amorphous phase appear. A 200 s collection time was used for acquiring the spectrum.

Other plasma-sprayed hydroxyapatite coatings, manufactured by independent coating vendors, were chosen for comparison. Because it is very difficult to avoid the amorphous-phase constituent, these coatings were expected to consist of an amorphous-phase constituent together with the crystalline hydroxyapatite.

Room-temperature CL microanalysis measurements were performed using an Oxford Instruments (Oxford, UK) MonoCL2 CL system attached to a Jeol (Tokyo, Japan) 35C SEM equipped with a Microspec (Tremont, CA, USA) wavelength dispersive X-ray spectrometer. The CL emission was collected using a diamond-machined paraboloidal mirror. Monochromatic CL images were collected using a Link (Oxford, UK) ISIS digital image capture system at 1024 × 800 pixels with 100 μs dwell time per pixel. The CL emission was dispersed using a 1200 lines/mm grating blazed at 500 nm and detected using a Hamamatsu (Japan) R943-02 Peltier cooled photomultiplier tube. CL spectra and monochromatic images were measured using accelerating voltages ranging from 15–35 keV and beam currents (measured using a Faraday cup) between 1 and 100 nA. All CL spectra were collected with a 5 nm bandpass, 5 nm step interval and a 1 s dwell time per step.

Flat surfaces were prepared either by polishing, fracture or utilizing the as-sprayed coating surface. Preparation stages for polished sections involved grinding on a 600 grit paper followed by polishing with 3, 1, and 0.25 μm diamond polishing compounds on a SIRO tin lap surface. The preferred elevation of the crystalline phase was achieved by polishing with a 0.05 μm gamma alumina.

3. Results and discussion

The X-ray diffraction of the ground coating presented a broad peak typical of the amorphous phase found in coatings manufactured by plasma spraying hydroxyapatite, Fig. 1. The remaining peaks were identified as those characteristic of hydroxyapatite. The amount of amorphous phase in this coating, calculated using an internal standard method, was found to be approximately 70 wt %. This represents the average amorphous phase content within the entire coating. The X-ray diffraction pattern for the sintered hydroxyapatite is given for comparison.

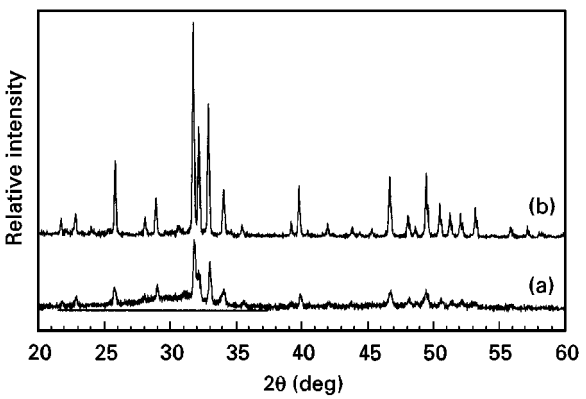

Figure 1 X-ray diffraction patterns of (a) a plasma-sprayed calcium phosphate coating containing an amorphous phase and hydroxyapatite, and (b) a sintered hydroxyapatite sample containing a small amount of tricalcium phosphate.

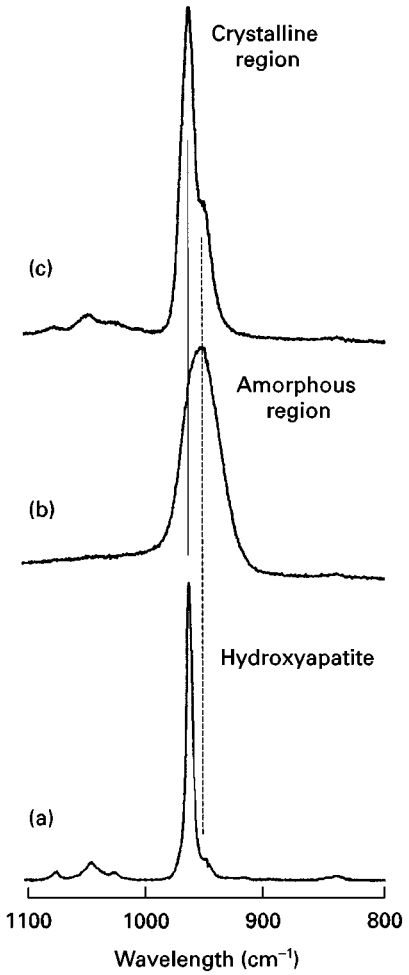

Figure 2 Microprobe Raman spectra of (a) sintered hydroxyapatite, (b) an amorphous region of the planar polished section of a hydroxyapatite coating, and (c) a crystalline region of the planar polished section of a hydroxyapatite coating.

Raman microprobe spectroscopy produces a broad peak at 950 cm^{-1} for the amorphous phase and narrow peak at 960 cm^{-1} for hydroxyapatite. This has been documented by Weinlaender *et al.* [10] who macroscopically analyzed a high amorphous content coating. The spectrum collected from the sintered hydroxyapatite shows a peak at 960 cm^{-1}, representative of hydroxyapatite, Fig. 2. Investigation of the coating on the microstructural level revealed raised plateaus which were lighter in color compared to the background. These plateaus have been previously reported in laboratory prepared [3] and commercially available [20] coatings as corresponding to the crystalline phase. A Raman microprobe analysis of the background area revealed a peak at 950 cm^{-1}, confirming the previous findings. The spectrum obtained from the raised plateau in the microstructure indicated that hydroxyapatite was the larger constituent with the amorphous calcium phosphate as the accompanying chemical phase. The combination of the two phases could arise from two sources. Firstly, because lamellae in the coating formed by well molten particles are less than 5 μm thick, and it is not known precisely how much material from each individual lamella is removed during polishing, the signal could arise from both the crystalline region and the underlying

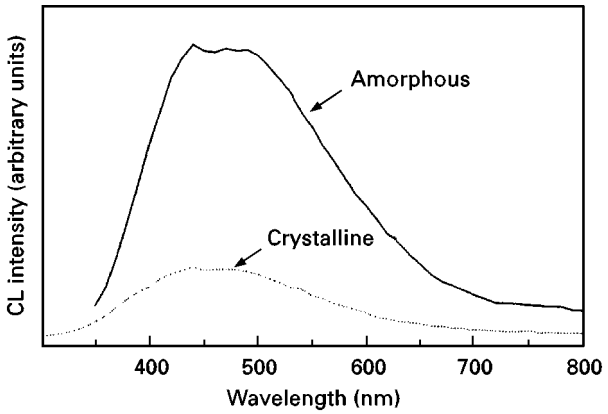

Figure 3 The cathodoluminescence emission from the amorphous-phase constituent and sintered hydroxyapatite.

amorphous phase region. Secondly, the crystalline regions are not necessarily smooth and so the response could incorporate some amorphous phase entrapped in the rough outer layer of the crystalline phase.

Cathodoluminescence spectroscopy of the amorphous phase yielded a broad emission ranging from 250–700 nm and centered around 450 nm, Fig. 3. The intensity was observed to occur at a markedly higher level compared to the crystalline phase. The emission appears to come from the same source, because upon normalization, the two curves overlap exactly.

Broad CL emission is often characteristic of defect centers [21]. Possible candidates in hydroxyapatite are the tetrahedral oxyanion (PO_4^{3-}), structural defects such as missing atomic species or substitutional impurities such as O^{2-} ions at hydroxyl sites. Further fundamental studies are required to assign the CL emission in hydroxyapatite to a particular luminescence center. Investigation of the CL emission as a function of temperature, excitation conditions (accelerating voltage and beam current) and time will provide useful information to assist in the identification of the CL center.

Because the broad emission is comparable for both structural phases, the panchromatic cathodoluminescence emission can be used to obtain a map of the amorphous phase. Analysis of a polished cross-section of a coating, where the distribution and location of the crystalline phases was observed in a secondary electron image, produced a direct correlation of the two phases in the cathodoluminescence image, Fig. 4. The brighter areas in the cathodoluminescence image correspond to the amorphous phase.

Various coatings produced by independent coating suppliers were analyzed and it was found that the same cathodoluminescence emission spectra were produced with a higher emission from the amorphous phase in all cases. This enabled the amorphous phase to be mapped in different coatings, signifying that the emission was a characteristic of the calcium phosphate which was more intense and not affected by the impurity elements in the coating. Another secondary image with the corresponding cathodoluminescence image is shown in Fig. 5.

The only correlation between a coating surface morphological entity and the amorphous phase has

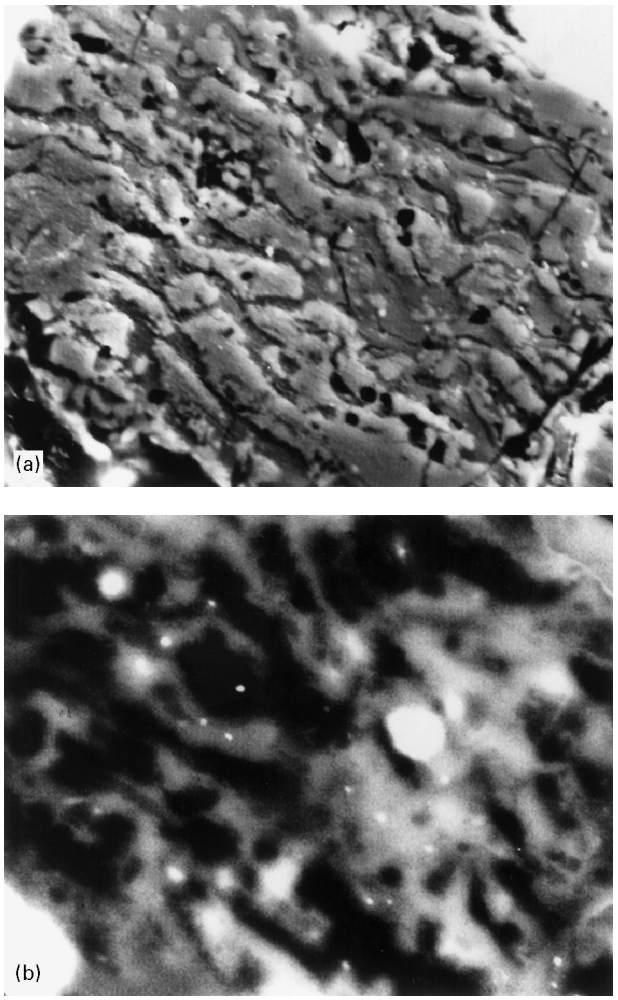

Figure 4 A polished coating viewed as a (a) secondary image, and (b) panchromatic cathodoluminescence image. The field of view in the horizontal direction is 180 μm.

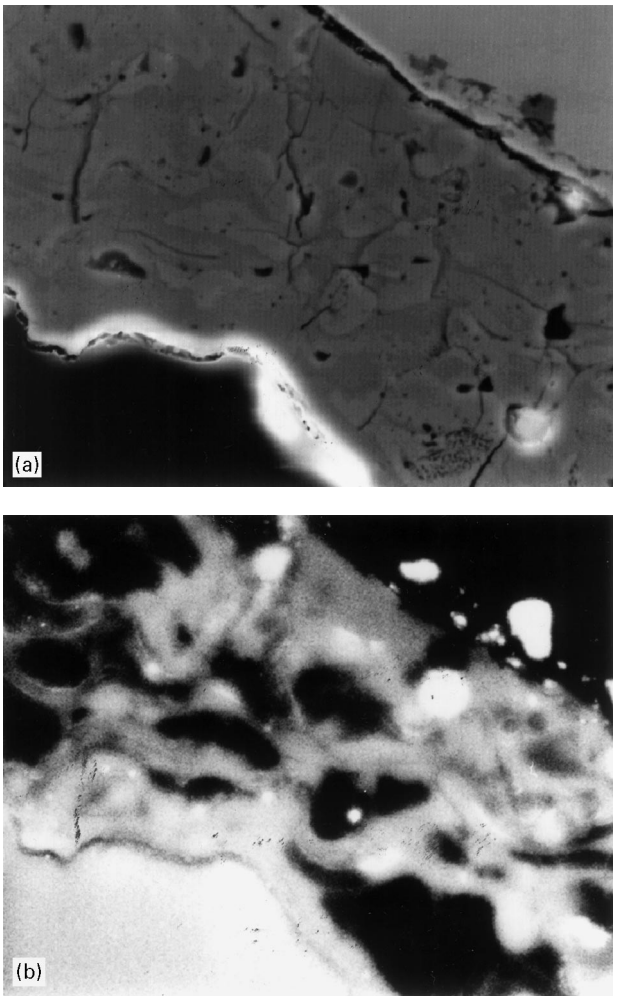

Figure 5 A polished coating viewed as a (a) secondary electron image, and (b) panchromatic cathodoluminescence image. The field of view in the horizontal direction is 180 μm.

been with a fine finger-like extension from a solidified particle [22]. This was ascertained using selected-area diffraction in a transmission electron microscope. Cathodoluminescence imaging, in conjunction with scanning electron microscopy, when applied to an as-sprayed surface, enabled an analysis of the entire coating surface. The secondary image shows fine particulate, lamellae corresponding to well molten particles, and partially molten particles, Fig. 6. The CL image indicates that most of the material located on the surface consists of the amorphous phase. Some lamellae of the same size are amorphous while other are crystalline. This suggests that it is not possible to correlate surface features to a particular phase by examination of the secondary image.

The fine particulate in different areas on the coating are crystalline which could arise from the core of partially molten particles. In most of the locations they have impacted the surface to produce scattered crystalline debris. One particle, marked with an arrow, shows a partially molten particle with a molten outer layer. The crystalline core produced the expected lower emission; however, the molten shell indicates that it consists of an amorphous phase. Oxyapatite could equally well form in this location because the heat withdrawal for this particle is significantly lower through the smaller contact area with the coating compared to a well molten particle. Other cathodoluminescence spectra of dehydroxylated hydroxyapatite not shown in this paper, did not show any difference with hydroxyapatite.

A further extension of this analysis tool enables the investigation of fracture surfaces. This allows the source of failure mechanisms to be investigated with respect to the amorphous phase without destroying the fractured coating. Fig. 7 shows a fracture cross-section with the CL image on the same area. The long elongated dark areas most likely represent crystallized lamellae.

An extension of this tool can be used in histological evaluation where thin sections are normally prepared to determine the bone attachment to the coating surface. With this technique no surface preparation is required, enabling direct analysis to determine whether the bone has attached preferentially to the amorphous or crystalline phases in the outer layer of the coating.

Photoluminescence using argon laser excitation has also been observed in hydroxyapatite coatings giving higher emission in certain parts of the coating microstructure [23]. During the Raman microprobe experiment on the amorphous-phase reference in this study, it was noted that the fluorescence was significantly higher compared to the crystalline phase.

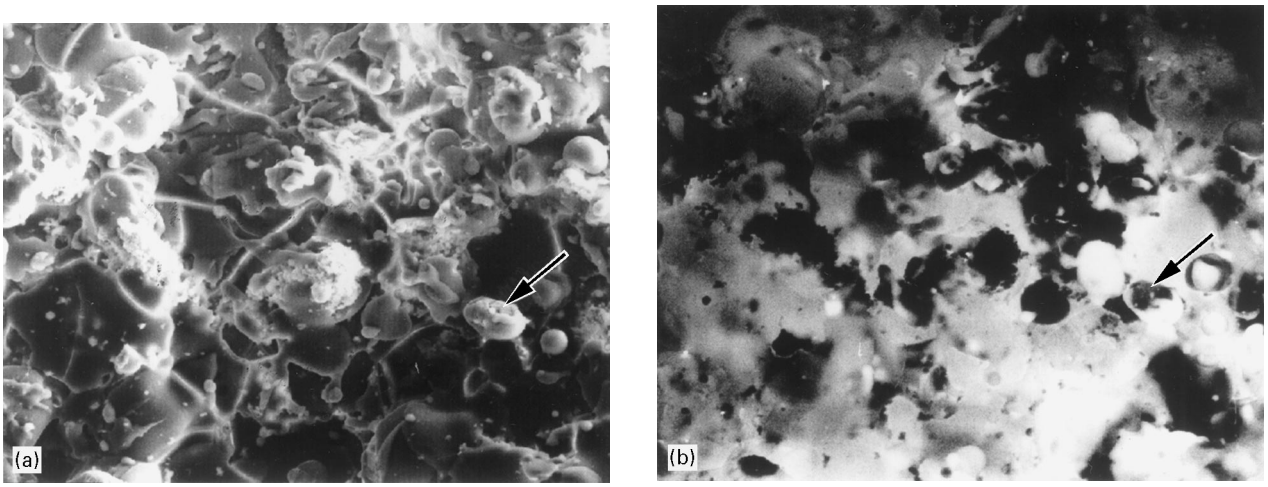

Figure 6 Surface view of an as-sprayed hydroxyapatite coating showing (a) a secondary electron image, (b) a panchromatic cathodoluminescence image. The field of view in the horizontal direction is 180 μm.

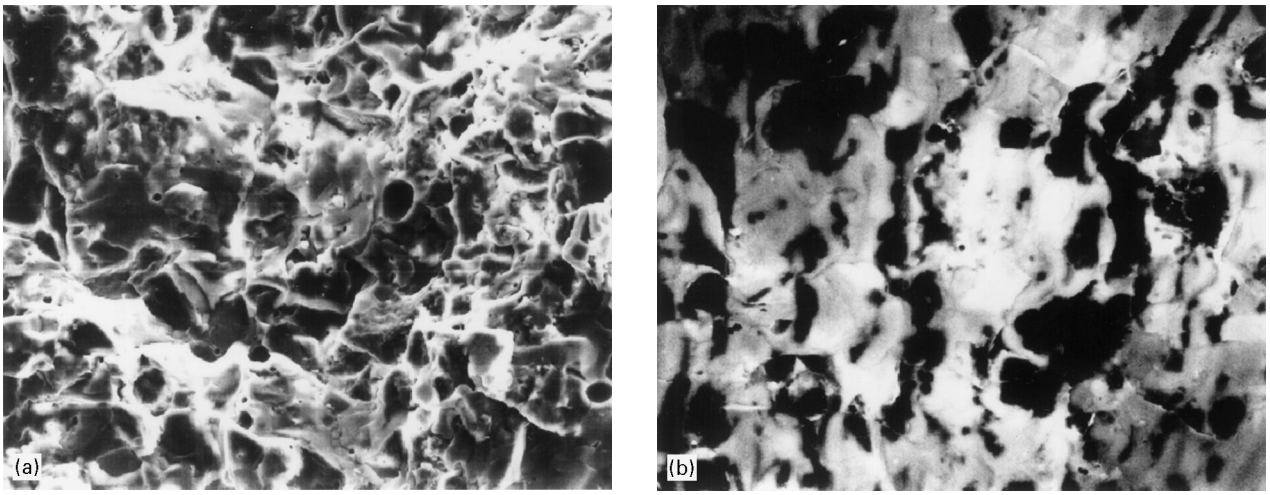

Figure 7 A fracture surface showing (a) a secondary electron image, and (b) a panchromatic cathodoluminescence image. The field of view in the horizontal direction is 180 μm.

Luminescence microscopy techniques such as confocal laser microscopy show promise for the characterization of coatings and the surrounding bone.

4. Conclusion

The stronger cathodoluminescence emission from the amorphous phase compared to hydroxyapatite enables amorphous-phase regions to be investigated without any surface preparation. Cathodoluminescence microscopy and analysis is a useful tool for identifying, locating and mapping the amorphous phase in calcium phosphate coatings. The added advantage of this technique is that as-sprayed surfaces and fracture surfaces can be investigated to determine the role of the amorphous phase in the performance of hydroxyapatite coatings.

Acknowledgments

The authors are grateful for access to a sintered hydroxyapatite article used as a standard supplied by The Division of Materials Science and Technology, The Commonwealth, Scientific and Industrial Research Organisation. Dr Karlis A. Gross acknowledges support provided by The Australian Research Council.

References

1. J. D. DE BRUIJN, T. P. BOVELL and C. A. VAN BLITTERSWIJK, *Biomaterials* **15** (1994) 543.
2. M. NAGANO, T. NAKAMURA, T. KOKUBO, M. TANAHASHI and M. OGAWA, *Biomaterials* **17** (1996) 1771.
3. K. A. GROSS, C. C. BERNDT, D. D. GOLDSCHLAG and V. J. IACONO, *Int. J. Oral Maxillofac. Implants* **12** (1997) 589.
4. C. Y. YANG, R. M. LIN, B. C. WANG, T. M. LEE, E. CHANG, Y. S. HANG and P. Q. CHEN, *J. Biomed. Mater. Res.* **37** (1997) 335.
5. J. S. FLACH, L. A. SHIMP, C. A. VAN BLITTERSWIJK and K. DE GROOT, in "Characterization and Performance of Calcium Phosphate Coatings for Implants, STP 1196" (American Society for Testing and Materials, Philadelphia, 1994) p. 25.
6. L. KELLER and P. REY-FESSLER, *ibid*., p. 54.
7. S. MAZUMDER and B. MUKHERJEE, *Mater. Res. Bull.* **30** (1995) 1439.

8. E. P. PASCHALIS, E. DICARLO, F. BETTS, P. SHERMANN, R. MENDELSOHN and A. L. BOSKEY, *Calcif. Tiss. Int*. **59** (1996) 480.
9. L. SAVARINO, S. STEA, D. GRANCHI, M. E. DONATI, M. CERVELLATI, A. MORONI, G. PAGANETTO and A. PIZZOFERRATO, *J. Mater. Sci. Mater. Med*. **9** (1988) 109.
10. M. WEINLAENDER, J. BEUMER, E. B. KENNEY, P. K. MOY and F. ADAR, *ibid*. **3** (1992) 397.
11. H. JI, C. B. PONTON and P. M. MARQUIS, *ibid*. **3** (1992) 283.
12. R. B. HEIMANN and T. A. VU, *J. Thermal Spray Technol*. **6** (1997) 145.
13. M. OGISO, Y. YAMASHITA and T. MATSUMOTO, *J. Biomed. Mater. Res*. **39** (1998) 23–31.
14. J. V. SMITH and R. C. STENSTROM, *J. Geol*. **73** (1965) 627.
15. A. M. PORTNOV and B. S. GOROBETS, *Dokl. Akad. Nauk. SSR* **184** (1969) 110.
16. R. H. MITCHELL, J. XIONG, A. N. MARIANO and M. E. FLEET, *Can. Mineral*. **35** (1997) 979.
17. A. S. MARFURIN, "Spectroscopy, Luminescence and Radiation Centres in Minerals" (Springer, Berlin, Heidelberg, New York, 1979).
18. A. M. MARIANO and P. J. RING, *Geochim. Cosmochim Acta* **39** (1975) 649.
19. K. A. GROSS, C. C. BERNDT and H. HERMAN, *J. Biomed. Mater. Res*. **39** (1998) 407–414.
20. K. A. GROSS, C. C. BERNDT and V. J. IACONO, *Int. J. Oral Maxillofac. Implants* (1998) in press.
21. B. G. YACOBI and D. B. HOLT, "Cathodoluminescence Microscopy of Inorganic Solids" (Plenum Press, New York, London, 1990).
22. S. J. YANKEE and B. J. PLETKA, in "Thermal Spray: International Advances in Coatings Technology", edited by C. C. Berndt (ASM International, Materials Park, OH, 1992) p. 453.
23. A. PIATTELLI and P. TRISI, *Biomaterials* **14** (1993) 973.

Received 7 May
and accepted 4 June 1998